

# Power-Imbalance Allocation Control of Power Systems-Secondary Frequency Control

Kaihua Xi, Johan L. A. Dubbeldam, Hai Xiang Lin, and Jan H. van Schuppen

**Abstract**—The traditional secondary frequency control of power systems restores nominal frequency by steering *Area Control Errors* (ACEs) to zero. Existing methods are a form of integral control with the characteristic that large control gain coefficients introduce an overshoot and small ones result in a slow convergence to a steady state. In order to deal with the large frequency deviation deviation problem, which is the main concern of the power system integrated with a large number of renewable energy, a faster convergence is crucial. In this paper, we propose a secondary frequency control method named *Power-Imbalance Allocation Control* (PIAC) to restore the nominal frequency with a minimized control cost, in which a coordinator estimates the power imbalance and dispatches the control inputs to the controllers after solving an economic power dispatch problem. The power imbalance estimation converges exponentially in PIAC, both overshoots and large frequency deviations are avoided. In addition, when PIAC is implemented in a multi-area controlled network, the controllers of an area are independent of the disturbance of the neighbor areas. Lyapunov stability analysis shows that PIAC is asymptotically stable and simulation results illustrates that it effectively eliminates the drawback of the traditional integral control based methods.

**Index Terms**—Power systems, Secondary frequency control, Economic power dispatch, Power imbalance, Overshoot, Large frequency deviation.

## I. INTRODUCTION

**R**APID expansion of the contribution of distributed renewable energy sources has accelerated research efforts in controlling the power grid. In general, frequency control is implemented at three different levels distinguished from fast to slow timescales [19], [13]. In a short time scale, the power grid is stabilized by the decentralized droop control, which is called *primary control*. While successfully balancing the power supply and demand, and synchronizing the power frequency, the primary control induces frequency deviations from the nominal frequency, e.g., 50 or 60 Hz. These deviations are reduced by the *Secondary frequency control* in a slower time scale than the primary control. On the top of the primary and secondary control, the *tertiary control* is concerned with global economic power dispatch over the networks in a large time scale. Consequently it depends on the energy prices and markets.

The secondary frequency control is the focus of this paper. An interconnected electric power system can be described as a collection of subsystems, each of which is called a control area. The secondary control in a single area is regulated by

*Automatic Generation Control* (AGC), which is driven by *Area Control Error* (ACE). The ACE of an area is calculated from the local frequency deviations within the area and power transfers between the area and its neighbor areas. The AGC controls the power injections to force the ACE to zero, thus restores the nominal frequency. Due to the availability of a communication network, other secondary frequency control approaches have recently been developed which minimize the control cost on-line [10], e.g., the Distributed Average Integral Method (DAI) [31], the Gather-Broadcast (GB) method [9], economic AGC (EAGC) method [15], and distributed real time power optimal power control method [17]. These methods suffer from a common drawback, namely that they exhibit overshoot for large gain coefficients and slow convergence for small gain coefficients. This is due to the fact that they rely on the integral control which is well-known to give rise to the two phenomena mentioned above. Note that the slow convergence speed results in a large frequency deviation which is the main concern of low inertia power systems.

The presence of fluctuations is expected to increase in the near future, due to the presence of generators with low inertia, such as solar and wind energy. This demonstrates the necessity of good secondary frequency control methods whose transient performance is enhanced with respect to the existing methods. We have recently derived such a method called *Power Imbalance Allocation Method* (PIAC) in [28], which can eliminate the drawback of the integral control based approach. This paper is the extended version of the conference paper [28] with additional stability analysis and the extension of PIAC to multi-area control.

We consider power systems with lossless transmission lines, which comprise traditional synchronous machines, frequency dependent power sources and passive loads. We assume the system to be equipped with the primary controllers and propose the PIAC method in the framework of Proportional-Integral (PI) control, which first estimates the power imbalance of the system via the measured frequency deviations of the nodes of the synchronous machines and frequency dependent power sources, next dispatches the control inputs of the distributed controllers after solving the economic power dispatch problem. Since the estimated power imbalance converges exponentially at a rate that can be accelerated by increasing the control gain coefficient, the overshoot problem and the large frequency deviation problem is avoided. Hence the drawback of the traditional ACE method is eliminated. Furthermore, the control gain coefficient is independent to the parameters of the power system but only relies on the response time of the control devices. Consequently the transient performance

Kaihua Xi, Johan L. A. Dubbeldam, Hai Xiang Lin and Jan H. van Schuppen are with Delft Institute of Applied Mathematics, Delft University of Technology, Mekelweg 4, 2628CD, Delft, The Netherlands. Email: (K.Xi, J.L.A.Dubbeldam, H.X.Lin, J.H.vanSchuppen)@tudelft.nl.

is greatly enhanced by improving the performance of the control devices in PIAC. When implemented in a multi-area power network, PIAC makes the control actions of the areas independent, while the controllers of each area handles the power imbalance of the local area only.

The paper is organized as follows. We introduce the mathematical model of the power system in section II. We formulate the problem and discuss the existing approaches in section III, then propose the secondary frequency control approach, *Power-Imbalance Allocation Control* (PIAC), based on estimated power imbalance in section IV and analyze its the stability invoking the Lyapunov/LaSalle stability criterion in section V. Finally, we evaluate the performance of PIAC by simulations on the IEEE-39 New England test power system in section VI. Section VII concludes with remarks.

## II. THE MODEL

A power system is described by a graph  $G = (\mathcal{V}, \mathcal{E})$  with nodes  $\mathcal{V}$  and edges  $\mathcal{E} \subseteq \mathcal{V} \times \mathcal{V}$ , where a node represents a bus and edge  $(i, j)$  represents the direct transmission line connection between node  $i$  and  $j$ . We consider a power system as a lossless electric network with constant voltage and an adjacency matrix  $(\hat{B}_{ij})$ , where  $\hat{B}_{ij}$  denotes the susceptance between node  $i$  and  $j$ . The system consists of three types of nodes, synchronous machines, frequency dependent devices and passive loads, the sets of which are denoted by  $\mathcal{V}_M$ ,  $\mathcal{V}_F$  and  $\mathcal{V}_P$  respectively. thus  $\mathcal{V} = \mathcal{V}_M \cup \mathcal{V}_P \cup \mathcal{V}_F$ . Denote the number of the nodes in  $\mathcal{V}$ ,  $\mathcal{V}_M$ ,  $\mathcal{V}_F$ ,  $\mathcal{V}_P$  by  $n$ ,  $n_M$ ,  $n_F$ , and  $n_P$  respectively, hence  $n = n_M + n_F + n_P$ . The model is described by the following *Differential Algebraic Equations* (DAEs), see e.g., [9],

$$M_i \ddot{\theta}_i + D_i \dot{\theta}_i = P_i - \sum_{j \in \mathcal{V}} B_{ij} \sin(\theta_i - \theta_j) + u_i, \quad i \in \mathcal{V}_M, \quad (1a)$$

$$D_i \dot{\theta}_i = P_i - \sum_{j \in \mathcal{V}} B_{ij} \sin(\theta_i - \theta_j) + u_i, \quad i \in \mathcal{V}_F, \quad (1b)$$

$$0 = P_i - \sum_{j \in \mathcal{V}} B_{ij} \sin(\theta_i - \theta_j), \quad i \in \mathcal{V}_P, \quad (1c)$$

where  $M_i > 0$  denotes the moment of inertia of a synchronous machine,  $D_i > 0$  the droop control coefficient,  $P_i$  the power injection or demand at node  $i$ ,  $B_{ij} = \hat{B}_{ij} V_i V_j$  the effective susceptance matrix,  $V_i$  the voltage at node  $i$ ,  $u_i \in [\underline{u}_i, \bar{u}_i]$  the control input. Note that  $u_i$  is a constraint control input of the secondary frequency control,  $\underline{u}_i$  and  $\bar{u}_i$  are its lower and upper bound, respectively. Furthermore, the set of nodes equipped with the secondary controllers is denoted by  $\mathcal{V}_K \subseteq \mathcal{V}_M \cup \mathcal{V}_F$  and  $u_i = 0$  for  $i \notin \mathcal{V}_K$ . Here, we have assumed that the nodes that participate in secondary control are equipped with primary controllers. Note that the loads can also be equipped with primary controllers [32]. The frequency deviation from the nominal frequency, i.e., 50 Hz or 60 Hz, is defined as

$$\omega_i = \dot{\theta}_i, \quad i \in \mathcal{V}_M \cup \mathcal{V}_F, \quad (2)$$

The dynamics of the reactive power and voltage dynamics is not modeled, since they are irrelevant for control of the frequency. More details on decoupling the voltage and frequency control can be found in [14] and [22].

## III. SECONDARY FREQUENCY CONTROL OF POWER SYSTEMS

### A. Problem formulation

In practice, the frequency deviation should be in a prescribed range in order to avoid damage to the devices in the power system. We assume droop controllers to be installed at some nodes such that  $\sum_{i \in \mathcal{V}_M \cup \mathcal{V}_F} D_i > 0$ . The explicit synchronized frequency deviation from the nominal frequency with droop control and secondary control is obtained as

$$\omega_{syn} = \frac{\sum_{i \in \mathcal{V}} P_i + \sum_{i \in \mathcal{V}_K} u_i}{\sum_{i \in \mathcal{V}_M \cup \mathcal{V}_F} D_i}, \quad (3)$$

If and only if  $\sum_{i \in \mathcal{V}} P_i + \sum_{i \in \mathcal{V}_K} u_i = 0$ , the frequency deviation of the steady state is zero, i.e.,  $\omega_{syn} = 0$ . This implies that a system with only droop control, i.e.,  $u_i = 0$ , for  $i \in \mathcal{V}_K$ , can never converge to a steady state with  $\omega_{syn} = 0$  if the power demand and supply is unbalanced such that  $\sum_{i \in \mathcal{V}} P_i \neq 0$ . This shows the need for the secondary control. We aim to control  $\omega_{syn}$  to zero by solving the following problem, e.g., [10] and [9].

**Problem 1.** Compute the inputs  $\{u_i, i \in \mathcal{V}_K\}$  of the power system so as to achieve the *control objective of a balance of power supply and demand* in terms of  $\omega_{syn} = 0$ , or equivalently,  $\sum_{i \in \mathcal{V}} P_i + \sum_{i \in \mathcal{V}_K} u_i = 0$ .

For a basic feasibility condition to solve Problem 1, we make two assumptions.

**Assumption 1.** The total amount of power imbalance can be compensated by the control inputs  $\{u_i, i \in \mathcal{V}_K\}$ , i.e.

$$-\sum_{i \in \mathcal{V}} P_i \in [\sum_{i \in \mathcal{V}_K} \underline{u}_i, \sum_{i \in \mathcal{V}_K} \bar{u}_i]. \quad (4)$$

Assumption 1 is realistic since the main task of the generators is to provide electricity to the loads and maintain the nominal frequency.

Furthermore, to ensure the existence of a steady state of the power system, we make a second assumption.

**Assumption 2.** During a small time interval the value of power supply and demand are constant. In addition, for these values there exist control inputs  $\{u_i \in [\underline{u}_i, \bar{u}_i], i \in \mathcal{V}_K\}$ , such that  $\sum_{i \in \mathcal{V}} P_i + \sum_{i \in \mathcal{V}_K} u_i = 0$ .

In the small time interval, the tertiary control, which calculates the operating point stabilized by the secondary control, guarantees the existence of a steady state and its local stability [13], [23]. Thus, Assumption 2 is also realistic.

For different controllers in the system, the control cost might be different for various reasons such as different device maintenance prices. From the global perspective of the entire network, we aim to minimize the secondary frequency control cost which leads to Problem 2.

**Problem 2.** Compute the inputs  $\{u_i, i \in \mathcal{V}\}$  of the power system so as to achieve the *control objective of minimal control cost*, in addition to the control objective of a balance of power supply and demand with  $\omega_{syn} = 0$ .

Corresponding to Problem 2, the following economic power dispatch problem needs to be solved[15].

$$\begin{aligned} \min_{u \in \mathbb{R}^{n_K}} \quad & \sum_{i \in \mathcal{V}_K} J_i(u_i) \\ \text{s.t.} \quad & \sum_{i \in \mathcal{V}} P_i + \sum_{i \in \mathcal{V}_K} u_i = 0. \end{aligned} \quad (5)$$

where  $J_i(u_i)$  is the control cost of the node  $i$ , which incorporate the cost money and the constraints  $u_i \in [\underline{u}_i, \bar{u}_i]$ . Note that to solve (5), the sum  $\sum_{i \in \mathcal{V}} P_i$  should be known and the solution is for the small time interval mentioned in Assumption 2. Here, With respect to the existence of the solution of the economic power dispatch problem, we make the third assumption.

**Assumption 3.** The cost functions  $J_i : \mathbb{R} \rightarrow \mathbb{R}$ ,  $i \in \mathcal{V}_K$  are twice continuously differentiable and strictly convex such that  $J''(u_i) > 0$  where  $J''(u_i)$  is the second order derivative of  $J(u_i)$  with respect to  $u_i$ .

Assumption 3 is also realistic because the constraint  $u_i \in [\underline{u}_i, \bar{u}_i]$  can be incorporated in the objective function  $J_i(u_i)$  for  $i \in \mathcal{V}_K$  in a smooth way,

A necessary condition for solving the economic dispatch problem is [13],

$$J'_i(u_i) = J'_j(u_j) = \lambda, \quad \forall i, j \in \mathcal{V}. \quad (6)$$

where  $J'_i(u_i)$  is the derivative of  $J_i(u_i)$ , which is the *marginal cost* of node  $i$ ,  $i \in \mathcal{V}_K$ , and  $\lambda \in \mathbb{R}$  is the *nodal price*. At the optimum of (5) all the marginal costs of the controllers are equal to the nodal price. The *market clearing price*  $\lambda^*$  is obtained as the solution of the equation

$$0 = \sum_{i \in \mathcal{V}} P_i + \sum_{i \in \mathcal{V}_K} J'^{-1}_i(\lambda^*). \quad (7)$$

where  $J'^{-1}_i(\cdot)$  is the inverse function of  $J'_i(\cdot)$  which exists by Assumption 3. Since in practice the power imbalance is uncertain with respect to the fluctuating power loads, the economic power dispatch problem (5) cannot be solved directly.

### B. A brief review of the secondary frequency control

Before embarking on solving Problem 1 and 2, we briefly outline existing secondary frequency control methods and discuss their relevance for finding a solution to problems 1 and 2.

**ACE based AGC[13]:** The *Area Control Error* (ACE) of an area is defined as

$$ACE = B\omega + P_{ex} - P_{ex}^*, \quad (8)$$

where  $B$  is a positive constant,  $\omega$  is the frequency deviation of the area,  $P_{ex}$  is the net power export, and  $P_{ex}^*$  is the nominal value of  $P_{ex}$ . The adjustment of the power injection of the area is given as follows

$$\dot{u} = -k \cdot ACE \quad (9)$$

where  $k$  is a positive control gain coefficient. In the traditional *Automatic Generation Control* (AGC) method, the frequency deviation is measured at a local node and communicated by a coordinator as the ACE to the controllers in the system, which calculate their control inputs according to their participation

factors. When the interconnected system is considered as a single area, the AGC has the form [9]

$$\dot{\lambda} = -k\omega_{i^*}, \quad i \in \mathcal{V}, \quad u_i = J'^{-1}_i(\lambda), \quad (10)$$

where  $k$  is a control gain coefficient,  $\omega_{i^*}$  is the measured frequency deviation at a selected node  $i^*$ . Note that  $\lambda$  can be seen as the nodal price which converges to the market clearing price  $\lambda^*$  as the power supply and demand is balanced. Note that the participation factor is involved in the derivative of the cost function,  $J'_i(u_i)$ . The frequency deviation of the area is not well reflected since it is measured at only one node. Furthermore, the communication network is not used so efficiently because it only communicates the nodal price  $\lambda$  from the coordinator to the controllers.

**Gather-Broadcast (GB) Control[9]:** In order to well reflect the frequency deviation of the area and use the communication network efficiently, the GB method measures the frequency deviations at all the nodes connected by the communication network. It has the form

$$\dot{\lambda} = -k \sum_{i \in \mathcal{V}} C_i \omega_i, \quad i \in \mathcal{V}, \quad u_i = J'^{-1}_i(\lambda), \quad (11)$$

where  $k$  is a control gain coefficient and  $C_i \in [0, 1]$  is a set of convex weighting coefficients with  $\sum_{i \in \mathcal{V}} C_i = 1$ . As in the ACE based AGC method, a coordinator in the network also broadcasts the nodal price to the controllers and the controllers compute the control inputs according to their own cost functions.

**Distributed Averaging Integral control (DAI):** Unlike the ACE base AGC method and GB method implemented in a centralized way, DAI is implemented in a distributed way based on the consensus control principle [1]. In the DAI method, there is no coordinator and each controller computes its own nodal price and communicates to its neighbors. A local node in the system calculates its control input according to the local frequency deviation and the nodal prices received from its neighbors. As the state of the interconnected system reaches a new steady state, the nodal prices of all the nodes consensus at the market clearing price, thus Problem 2 is solved. It has the form [31]

$$\dot{\lambda}_i = k_i(-\omega_i + \sum_{j \in \mathcal{V}} w_{ij}(\lambda_j - \lambda_i)), \quad u_i = J'^{-1}_i(\lambda_i). \quad (12)$$

where  $k_i$  is a gain coefficient for the controller  $i$  and  $(w_{ij})$  denotes the undirected weighted communication network. The DAI control has been widely studied on both the traditional power grids and Micro-Grids, e.g., [21], [6]. Note that,  $\omega_i$  is the frequency deviation of node  $i$  from the nominal frequency which should be known for nodes in  $\mathcal{K}$ . Wu *et.al.* [26] proposed a distributed secondary control method where it is not necessary to know the nominal frequency for all the nodes in  $\mathcal{K}$ .

When a steady state exists for the nonlinear system (1a-1c), all the approaches above can restore the nominal frequency with an optimized control cost. However, a common drawback is that the transient performance suffers from an overshoot problem or slow convergence speed since the methods are actually integral control methods. For a view of the overshoot,

we refer to the simulation results in section VI.

The methods that we discussed above, concern controlling the nonlinear system (1a-1c). However, the linearized version of the evolution equations (1a-1c) was also addressed in the literature. For example, Li *et al.* proposed an Economic AGC (EAGC) approach for the multi-area frequency control [15]. In this method each controller exchanges control signals that are used to successfully steer the state of the system to a steady state with optimized dispatch, by a partial primal-dual gradient algorithm [4]. Unfortunately, transient performance was not considered in the method. A potentially very promising method to the control of the linear system was recently proposed by Zhao *et al.* In [30] a novel framework for primary and secondary control, which we call Unified Control (UC), was developed. The advantage of UC is that it automatically takes care of the congestions that may occur in the transmission lines. Numerical simulations results show that the UC can effectively reduce the harmful large transient oscillations in the frequency. However, so far a theoretical analysis on how the UC improves the transient performance is lacking. Another recently reported study is by Liu *et al.* in [17]. They investigated a distributed real-time optimal power flow control of power systems, a the same providing the stability analysis. This method optimizes both control costs and manages power flow congestion using the principle of consensus control, but cannot prevent large frequency deviations at short times.

Finally, we mention here control methods whose underlying principle is not based on integral control. The optimal load-frequency control framework by Liu *et al.*, described in [16], is an example of such a method. The goal is still to optimize the control costs and frequency deviation, but rephrasing it as a finite horizon optimization problem. This can only be solved when the loads are precisely known within the selected time horizon. Obviously, this will require very precise forecasting of the loads. A more robust approach based on the concept of the Active Disturbance Rejection Control (ADRC) [11], was pursued by Dong *et al.* [7]. The method is robust against model uncertainties, parameter variations and large perturbations which was employed to construct a decentralized load frequency approach for interconnected systems. However, the decentralized control employed in this method prevents a solution to Problem 2.

As more renewable power sources are integrated into the power system, the fluctuations in the power supply become faster and larger. There is a need to design a control law that has a good transient performance without the overshoot problem and with a fast convergence speed. The traditional method to eliminate the overshoot is to calculate the control gain coefficients by analyzing the eigenvalue of the linearized systems [25], [24]. However, since the eigenvalues depend on the structure of the control methods, the improvement of the transient performance obtained by the eigenvalue analysis is not as good as expected.

Based on the framework of PI control this paper aims to design a secondary frequency control method that remedies the drawbacks mentioned above of the existing methods. To this end we formulate 4 requirements that we consider essential/beneficial for developing the controller that we propose:

- (i) The secondary frequency control cost should be minimized.
- (ii) The marginal costs of all controllers are identical during the transient phase.
- (iii) The frequency overshoot due the controller inputs must be close to zero.
- (iv) The number of parameters of should be small.

#### IV. POWER IMBALANCE ALLOCATION CONTROL

In this section, with four requirements listed in section III, we propose a secondary frequency control approach, named Power-Imbalance Allocation Control (PIAC), to solve Problem 1 and 2. Before introducing the approach, we make another assumption beside the assumptions 1-3,

**Assumption 4.** All the buses in  $\mathcal{V}_M \cup \mathcal{V}_F$  can communicate with a coordinator at a central location via a communication network. The frequency deviations  $\{\omega_i, i \in \mathcal{V}_M \cup \mathcal{V}_F\}$  can be measured and subsequently communicated to the coordinator. The control inputs  $\{u_i, i \in \mathcal{V}_K\}$  can be computed by the coordinator and dispatched to the controller at node  $i$ , for all  $i \in \mathcal{V}_K$ .

The control law is based on the design principle of coordination. The local nodes in  $\mathcal{V}_M \cup \mathcal{V}_F$  measure the frequency deviations and send them to the coordinator. The coordinator computes the control inputs  $\{u_i, i \in \mathcal{V}_K\}$  using the local measurements and sends them to all local controllers of the nodes indexed by  $\mathcal{V}_K$ . The coordination control has a beneficial effect on the stability of the frequency control of the power system and on the minimization of the economic cost. The procedure is similar to the Gather-Broadcast control which gathers the locally measured frequency deviation from the nodes and broadcasts the nodal price to the controllers. However, PIAC broadcasts the control inputs  $\{u_i, i \in \mathcal{V}_K\}$  to all the controllers. The PIAC method attempts to avoid unnecessary oscillations of the state and of the inputs.

In the following, we first introduce the PIAC method implemented in the networks with a single area to simplify the expression, then in the networks with multiple areas.

##### A. Single-area implementation of PIAC

Assume the network is controlled as a single area. The control procedure is mainly done by the coordinator. Besides collecting the measured frequency deviations and communicating the control inputs to the distributed controllers, the coordinator needs to do the following two tasks: (a) estimating the power imbalance  $\sum_{i \in \mathcal{V}} P_i$  on-line, (b) solving the economic power dispatch problem for the required power injection of all controllers,  $\{u_i, i \in \mathcal{V}_K\}$ .

The details of the two tasks are as follows.

- (a). On-line estimation of the power imbalance.

Define

$$z(t) = - \sum_{i \in \mathcal{V}_M} M_i \omega_i - \sum_{i \in \mathcal{V}_M \cup \mathcal{V}_F} \int_0^t D_i \omega_i(s) ds, \quad (13)$$

which can be computed by the coordinator after gathering the measured frequency deviations  $\{\omega_i, i \in \mathcal{V}_M \cup \mathcal{V}_F\}$ . Summing (1a-1c), we obtain

$$\sum_{i \in \mathcal{V}_M} M_i \dot{\omega}_i = \sum_{i \in \mathcal{V}} P_i - \sum_{i \in \mathcal{V}_M \cup \mathcal{V}_F} D_i \omega_i + \sum_{i \in \mathcal{V}_K} u_i. \quad (14)$$

which yields

$$\dot{z}(t) = - \sum_{i \in \mathcal{V}} P_i - \sum_{i \in \mathcal{V}_K} u_i(t). \quad (15)$$

With a positive  $k \in \mathbb{R}$ , define  $u_s(t) = kz(t)$ , which is taken as the sum  $\sum_{i \in \mathcal{V}_K} u_i(t)$ , then by (15),

$$\dot{z}(t) = - \sum_{i \in \mathcal{V}} P_i - u_s(t) = - \sum_{i \in \mathcal{V}} P_i - kz(t) \quad (16)$$

Since  $k$  is positive,  $k \in (0, +\infty)$ , then  $kz(t)$  converges to  $-\sum_{i \in \mathcal{V}} P_i$  exponentially, thus  $-kz(t)$  is an estimate of the power imbalance. Furthermore, the convergence speed of  $kz(t)$  only relies on the coefficient  $k$  which is independent to the parameters of the power system. Note that  $kz(t)$  can still track Lipschitz continuous time-varying power imbalance closely with a large gain coefficient  $k$  [29].

(b) Calculation of the control inputs  $\{u_i, i \in \mathcal{V}_K\}$  of the controllers.

With the estimated power imbalance  $-kz(t) \approx \sum_{i \in \mathcal{V}} P_i$ , the following optimization problem is solved as an alternative to (5).

$$\begin{aligned} \min_{u_i \in \mathbb{R}} \quad & \sum_{i \in \mathcal{V}_K} J_i(u_i), \\ \text{s.t.} \quad & -kz(t) + \sum_{i \in \mathcal{V}_K} u_i = 0. \end{aligned} \quad (17)$$

which is solved directly by the coordinator.

The control procedure of PIAC is summarized as follows.

**Procedure 2.1:** With the assumption 1-4 hold, the secondary frequency control approach of the power system (1), PIAC, is implemented as follows.

(i) Collect the measured frequency deviations

$$\{\omega_i, i \in \mathcal{V}_M \cup \mathcal{V}_F\},$$

(ii) Calculate the value  $z(t)$  by (13),

(iii) Solve the optimization problem (17),

(iv) Allocate the power compensation  $\{u_i, i \in \mathcal{V}_K\}$  to the controllers.

The solution of the optimization problem (17) is

$$u_i = J_i'^{-1}(\lambda)$$

for  $i \in \mathcal{V}_K$  where  $J_i'^{-1}(\cdot)$  is the inverse of  $J_i'(\cdot)$  and the nodal price  $\lambda$  is solved from

$$\sum_{i \in \mathcal{V}_K} J_i'^{-1}(\lambda) - kz(t) = 0.$$

The closed loop system of PIAC is

$$\dot{\theta}_i = \omega_i, \quad i \in \mathcal{V}_M \cup \mathcal{V}_F, \quad (18a)$$

$$M_i \dot{\omega}_i = P_i - D_i \omega_i - \sum_{j \in \mathcal{V}} B_{ij} \sin(\theta_{ij}) + J_i'^{-1}(\lambda), \quad i \in \mathcal{V}_M, \quad (18b)$$

$$0 = P_i - D_i \omega_i - \sum_{j \in \mathcal{V}} B_{ij} \sin(\theta_{ij}) + J_i'^{-1}(\lambda), \quad i \in \mathcal{V}_F, \quad (18c)$$

$$0 = P_i - \sum_{j \in \mathcal{V}} B_{ij} \sin(\theta_{ij}), \quad i \in \mathcal{V}_P, \quad (18d)$$

$$\dot{\eta} = \sum_{i \in \mathcal{V}_M \cup \mathcal{V}_F} D_i \omega_i, \quad (18e)$$

$$0 = \sum_{i \in \mathcal{V}_K} J_i'^{-1}(\lambda) + k \left( \sum_{i \in \mathcal{V}_M} M_i \omega_i + \eta \right), \quad (18f)$$

$$0 = J_i'^{-1}(\lambda), \quad i \notin \mathcal{V}_K. \quad (18g)$$

where  $\theta_{ij} = \theta_i - \theta_j$ . Note that  $\eta$  is a state variable introduced for the integral term in (13), and  $\lambda$  is an algebraic variable for solving the optimization problem (17), which is a function of time.

As will be proven in the remainder of the paper, PIAC satisfies the four requirements listed in section III.

- (i) As the state converges to a steady state and the nodal price  $\lambda$  converges to the market clearing price  $\lambda^*$ , the control cost is minimized.
- (ii) The optimization problem is solved on-line. By (18f), the marginal cost of all the controllers are identical during the transient phase.
- (iii) By the first-order differential equation (16),  $-kz(t)$  converges to the power imbalance exponentially. Thus the overshoot problem and the large frequency deviation problem is avoided.
- (iv) In the network as a single area, only one parameter, the gain coefficient  $k$ , needs to be determined. Moreover, the coefficient  $k$  does neither depend on the parameters of the systems nor on the economic power dispatch problem.

PIAC is actually a centralized control method. The communicated data include dynamic data and static data. The dynamic data are the frequency deviations  $\{\omega_i, i \in \mathcal{V}_M \cup \mathcal{V}_F\}$  and the control inputs  $\{u_i, i \in \mathcal{V}_K\}$ , both should be communicated frequently. The static data are the inertia of moment  $\{M_i, i \in \mathcal{V}_i\}$ , the droop control coefficients  $\{D_i, i \in \mathcal{V}_M \cup \mathcal{V}_F\}$  and the cost functions  $\{J_i(u_i), i \in \mathcal{V}_K\}$ , which are constant in a short time as in Assumption 2 and are not necessary to communicate as frequently as the dynamic data.

Solving the optimization problem (17) is equivalent to solving the equations (18e) and (18f), so the computation includes calculating the integral of frequency deviation in (18e) and solving the algebraic equation ((18f)). For quadratic cost functions  $J_i(u_i) = u_i^2/\alpha_i$ , the computing amounts approximately  $4n_M + n_F$  arithmetic operations that are  $*$ ,  $+$ ,  $-$  etc. For nonlinear cost functions, iteration method is used to solve the one dimension nonlinear algebraic equation ((18f)), which needs more computing than for the quadratic cost functions.

By (16), the estimation of the power imbalance converges exponentially in a speed that can be accelerated by increasing the control gain coefficient  $k$  which does not depend on any parameters of the power system and the cost functions. Hence, when the dynamics of the voltages are considered, the power supply and demand can also be balanced.

The control gain coefficient can be set very large from the perspective of theoretical analysis and it relies on how sensitive the control devices are to the fluctuation of power imbalance. In this case, it can be tuned according to the response time of the control devices and the desired range of the frequency deviation.

If there are no synchronous machines, i.e.,  $\mathcal{V}_M = \emptyset$ , the control inputs will still converge to the power imbalance exponentially. Hence, PIAC also works for the secondary frequency control of Micro-Grids without the synchronous machines.

In the network as a single control area, by Assumption 4, the PIAC method requires that all the nodes in  $\mathcal{V}_M \cup \mathcal{V}_F$  can communicate with the coordinator. However, our initial numerical experiments show that PIAC can still restore the nominal frequency, where the estimated power imbalance converges to the actual power imbalance although not exponentially. This is because PIAC includes the integral control which drives the synchronized frequency deviation to zero.

In practice, the state of the power system is never at a true equilibrium state, because of the fluctuating of the power imbalance caused by the power loads. Furthermore, the fluctuating becomes even more serious as a large amount of renewable power sources are integrated into the power system. In this case, it is more practical to model the power imbalance as a time-varying function. For the power system with time-varying power imbalance, analysis and numerical simulations show that PIAC is also able to effectively control the frequency to any desired range by increasing the control gain coefficient  $k$  [29].

### B. Multi-area implementation of PIAC

In the multi-area control of the power system, the power export (import) of an area should equal to the nominal value calculated by the tertiary control. Denote the set of the nodes in the area  $A_r$  by  $\mathcal{V}_{A_r}$ , the set of the boundary lines between the area  $A_l$  and all the other areas by  $\mathcal{E}_{A_r}$ . Denote  $\mathcal{V}_{M_r} = \mathcal{V}_M \cap \mathcal{V}_{A_r}$  and  $\mathcal{V}_{F_r} = \mathcal{V}_F \cap \mathcal{V}_{A_r}$ . The multi-area control of PIAC in the area  $A_r$  can be implemented as follows.

$$\dot{\eta}_l = \sum_{i \in \mathcal{V}_{M_r} \cup \mathcal{V}_{F_r}} D_i \omega_i + P_{ex} - P_{ex}^*, \quad (19a)$$

$$0 = \sum_{i \in \mathcal{V}_K} J_i'^{-1}(\lambda_r) + k_l \left( \sum_{i \in \mathcal{V}_{M_r}} M_i \omega_i + \eta_r \right), \quad (19b)$$

$$u_i = J_i'^{-1}(\lambda_r), \quad i \in \mathcal{V}_{M_r} \cup \mathcal{V}_{F_r}. \quad (19c)$$

where  $P_{ex} = \sum_{i \in \mathcal{V}_{A_r}, (i,j) \in \mathcal{E}_{A_r}} B_{ij} \sin(\theta_{ij})$  is the export power of the area  $A_r$ , and  $P_{ex}^*$  is the nominal value of  $P_{ex}$ . We remark that the control gain coefficient  $k_r$  can be different for each area, which can be tuned according to the sensitivity of the control devices in the area. Note that the sum of the three terms in the right hand of (19a) is actually the ACE of the

area  $A_l$ . By (19a), as the synchronous frequency deviation is steered to zero,  $P_{ex}$  also converges to the nominal value  $P_{ex}^*$ . Let  $z_r = -\sum_{i \in \mathcal{V}_{M_r} \cup \mathcal{V}_{F_r}} u_i / k_r$ , then  $z_r(t) = \sum_{i \in \mathcal{V}_{M_r}} M_i \omega_i + \eta_r$ , similar as the derivation of (16), it yields

$$\dot{z}_r = - \sum_{i \in \mathcal{V}_{A_r}} P_i + P_{ex}^* - k_r z_r(t)$$

which indicates that the controllers in area  $A_r$  only respond to the power imbalance  $\sum_{i \in \mathcal{V}_{A_r}} P_i$ . Hence, in the network, the control actions of all the areas can be done in an asynchronous way where each area can balance the local power supply-demand at any time according to the availability of the devices.

In particular, PIAC becomes a decentralized control method if each node is seen as a single area and  $\mathcal{V}_P = \emptyset$ ,  $\mathcal{V}_K = \mathcal{V}_M \cup \mathcal{V}_F$ , i.e., for all  $i \in \mathcal{V}_M \cup \mathcal{V}_F$ ,

$$\dot{\eta}_i = D_i \omega_i + \sum_{j \in \mathcal{V}} B_{ij} \sin(\theta_{ij}) - \sum_{j \in \mathcal{V}} B_{ij} \sin(\theta_{ij}^*), \quad (20a)$$

$$u_i = -k_i(M_i \omega + \eta_i). \quad (20b)$$

where  $\{\theta_i^*, i \in \mathcal{V}\}$  are the steady state calculated by the tertiary control. Since  $u_i$  is tracking  $-P_i + \sum_{j \in \mathcal{V}} B_{ij} \sin(\theta_{ij}^*)$ , each node compensates the power imbalance locally and the control actions of the nodes are irrelevant to each other. However, the control cost is not optimized by the decentralized control method.

## V. STABILITY ANALYSIS OF PIAC

In this section, we analyze the stability of PIAC with the Lyapunov-LaSalle approach. The stability proof makes use of Theorem A.1 stated in the Appendix.

As indicated in subsection IV-B, the control actions of the areas are decoupled in the multi-area control network. So we only need to prove the stability of PIAC implemented in a single-area network. Extension to multi-area control networks then follows immediately.

We denote the angles in the sets  $\mathcal{V}_M, \mathcal{V}_F, \mathcal{V}_P$  by vectors  $\theta_M, \theta_F, \theta_P$ , the frequency deviations by vectors  $\omega_M, \omega_F, \omega_P$ , the angles in  $\mathcal{V}$  by  $\theta = (\theta_M^T, \theta_F^T, \theta_P^T)^T$ , and the frequency deviations by  $\omega = (\omega_M^T, \omega_F^T, \omega_P^T)^T$ .

Note that the closed system may not have a synchronous state if the power injections  $\{P_i, i \in \mathcal{V}\}$  are much larger than the line capacity  $B_{ij}$ . For more details of the synchronous state of the power system, we refer to [27], [8]. Therefore, we make the assumption 5.

**Assumption 5:** For the closed loop system (18), there exists a synchronous state  $(\theta^*, \omega^*, \eta^*, \lambda^*) \in \mathbb{R}^n \times \mathbb{R}^n \times \mathbb{R} \times \mathbb{R}$  with  $\omega_i^* = \omega_{syn}$  and

$$\theta^*(t) \in \Theta = \{\theta \in \mathbb{R}^n \mid |\theta_i - \theta_j| < \frac{\pi}{2}, \quad \forall (i, j) \in \mathcal{E}\}.$$

The condition  $\theta^* \in \Theta$  is commonly referred to as a security constraint [6] in power system analysis. It can be satisfied by reserving some margin of power flow when calculating the operating point in the tertiary control [13].

Since the power flows  $\{B_{ij} \sin(\theta_i - \theta_j), (i, j) \in \mathcal{E}\}$  only depend on the angle differences and the angles can be expressed

relative to a reference node, we choose a reference angle, i.e.,  $\theta_1$ , in  $\mathcal{V}_M$  and introduce the new variables

$$\varphi_i = \theta_i - \theta_1, \quad i = 1, 2, \dots, n$$

which yields  $\dot{\varphi}_i = \omega_i - \omega_1$ . Note that  $\varphi_1 = 0, \dot{\varphi}_1 = 0$  for all  $t > 0$ . With  $\omega_i = \dot{\varphi}_i + \omega_1$  for  $i \in \mathcal{V}_F$ , the closed loop system (18) can be written in the DAE form as (31) in the Appendix,

$$\dot{\varphi}_i = \omega_i - \omega_1, \quad i \in \mathcal{V}_M \quad (21a)$$

$$M_i \dot{\omega}_i = P_i - D_i \omega_i - \sum_{j \in \mathcal{V}} B_{ij} \sin(\varphi_{ij}) + J_i'^{-1}(\lambda), \quad i \in \mathcal{V}_M, \quad (21b)$$

$$D_i \dot{\varphi}_i = P_i - D_i \omega_1 - \sum_{j \in \mathcal{V}} B_{ij} \sin(\varphi_{ij}) + J_i'^{-1}(\lambda), \quad i \in \mathcal{V}_F, \quad (21c)$$

$$0 = P_i - \sum_{j \in \mathcal{V}} B_{ij} \sin(\varphi_{ij}), \quad i \in \mathcal{V}_P, \quad (21d)$$

$$\dot{\eta} = \sum_{i \in \mathcal{V}_M \cup \mathcal{V}_F} D_i \omega_i, \quad (21e)$$

$$0 = \sum_{i \in \mathcal{V}_K} J_i'^{-1}(\lambda) + k \left( \sum_{i \in \mathcal{V}_M} M_i \omega_i + \eta \right), \quad (21f)$$

where  $\varphi_{ij} = \varphi_i - \varphi_j$ , and the equations (21a-21d) are from the power system and (21e-21f) from the controllers. We next recast the system (21) into the form of the DAE system (31), the state variables are  $x = (\varphi_M, \varphi_F, \omega_M, \eta) \in \mathbb{R}^{n_M-1} \times \mathbb{R}^{n_F} \times \mathbb{R}^{n_M} \times \mathbb{R}$ , the algebraic variables are  $y = (\varphi_P, \lambda) \in \mathbb{R}^{n_P} \times \mathbb{R}$ , the differential equations are (21a-21c, 21e) and the algebraic equations are (21d, 21f). Here  $\varphi_M$  is with the components  $\{\varphi_i, i \in \mathcal{V}_M\}$  besides  $\varphi_1$  which is a constant,  $\varphi_F$  with components  $\{\varphi_i, i \in \mathcal{V}_F\}$ , and  $\varphi_P$  with components  $\{\varphi_i, i \in \mathcal{V}_P\}$ . Note that the variables  $\{\omega_i, i \in \mathcal{V}_F\}$  are not included into the state variable or algebraic variables since the terms  $\{D_i \omega_i, i \in \mathcal{V}_F\}$  in (21e) can be replaced by  $\{P_i - \sum_{j \in \mathcal{V}} B_{ij} \sin(\varphi_{ij}) + J_i'^{-1}(\lambda), i \in \mathcal{V}_F\}$ . (18g) is neglected since it is irrelevant to the following stability analysis.

When mapping  $\theta$  to the coordinate of  $\varphi$ , assumption 5 yields

$$\varphi \in \Phi = \{\varphi \in \mathbb{R}^n \mid |\varphi_i - \varphi_j| < \frac{\pi}{2}, \quad \forall (i, j) \in \mathcal{E}, \text{ and } \varphi_1 = 0\}.$$

We remark that each equilibrium state of (21) corresponds to a synchronous state of (18). In the new coordinate, we have the following theorem for the stability of the system (21).

**Theorem 5.1:** If the assumptions 1-5 hold, then for the system (21),

- (a) there exists a unique equilibrium state  $z^* = (\varphi^*, \omega_M^*, \eta^*, \lambda^*) \in \Psi$  where  $\Psi = \Phi \times \mathbb{R}^{n_M} \times \mathbb{R} \times \mathbb{R}$ .
- (b) there exists a domain  $\Psi^d \subset \Psi$  such that for any initial state  $z^0 \in \Psi^d$  that satisfies the algebraic equations (21d) and (21f), the state trajectory converges to the unique equilibrium state  $z^* \in \Psi$ .

Note that the size of the attraction domain of the equilibrium state  $z^*$  is not determined in Theorem 5.1 which states the stability of the PIAC method. The proof of Theorem 5.1 is based on the Lyapunov/LaSalle stability criterion as in Theorem A.1. In the following, we first present the verification of the Assumption A.2 and A.3 in the Appendix for the DAE

system (21), then prove the stability of (21) by designing a Lyapunov function as  $V(x, y)$  in Theorem A.1. Lemma 5.2 states that (21) possesses an equilibrium state, which verifies Assumption A.2, and Lemma 5.3 claims the regularity of the algebraic equation (21d, 21f), which verifies Assumption A.3.

**Lemma 5.2:** There exists at most one equilibrium state  $z^* = (\varphi^*, \omega_M^*, \eta^*, \lambda^*)$  of the system (21) such that  $z^* \in \Psi$  and

$$\omega_i^* = 0, \quad i \in \mathcal{V}_M, \quad (22a)$$

$$\sum_{i \in \mathcal{V}} P_i + \sum_{i \in \mathcal{V}_K} J_i'^{-1}(\lambda^*) = 0. \quad (22b)$$

$$\sum_{i \in \mathcal{V}} P_i - k \eta^* = 0. \quad (22c)$$

*Proof:* At the synchronous state, by (16) it follows that

$$k \left( \sum_{i \in \mathcal{V}_M} M_i \omega_i^* + \eta^* \right) = \sum_{i \in \mathcal{V}} P_i.$$

Substitution into the algebraic equation (21f) yields (22b).

Substitution of (22b) in to (3) with  $u_i = J_i'^{-1}(\lambda)$ , we obtain  $\omega_{syn} = 0$  which yields  $\{\omega_i^* = 0, i \in \mathcal{V}_M\}$ . Hence

$$\sum_{i \in \mathcal{V}_K} J_i'^{-1}(\lambda^*) + k \eta^* = 0.$$

Subsequently this leads to (22c). It follows from [2] that the system (18) has at most one power flow solution such that  $\theta \in \Theta$ . Hence there exists at most one equilibrium for the system (21) that satisfies  $\varphi \in \Phi$ .  $\square$

With respect to the regularity of the algebraic equations (21d, 21f), we derive the following lemma.

**Lemma 5.3:** For any  $\varphi \in \Phi$  and strictly convex functions of  $\{J_i(u_i), i \in \mathcal{V}_K\}$  in the optimization problem (5), the algebraic equations (21d, 21f) are regular.

*Proof:* Since (21d) and (21f) are independent algebraic equations with respect to  $\varphi_P$  and  $\lambda$  respectively, the regularity of each of them is proven separately.

First, we prove the regularity of (21d) by showing that its Jacobian is a principle minor of the Laplacian matrix of a weighted network. In the coordination of  $\theta$ , we define function

$$\bar{U}(\theta) = \sum_{(i,j) \in \mathcal{E}} B_{ij} (1 - \cos(\theta_i - \theta_j)).$$

The Hessian matrix of  $\bar{U}(\theta)$  is

$$\bar{L} = \begin{pmatrix} \bar{B}_{11} & -B_{12} \cos(\theta_{12}) & \dots & -B_{1n} \cos(\theta_{1n}) \\ -B_{21} \cos(\theta_{12}) & \bar{B}_{22} & \dots & -B_{2n} \cos(\theta_{2n}) \\ \vdots & \vdots & \ddots & \vdots \\ -B_{n1} \cos(\theta_{n1}) & -B_{n2} \cos(\theta_{n2}) & \dots & \bar{B}_{nn} \end{pmatrix},$$

where  $\bar{B}_{ii} = \sum_{j \in \mathcal{V}} B_{ij} \cos(\theta_{ij})$  and  $\theta_{ij} = \theta_i - \theta_j$ .  $\bar{L}$  is the Laplacian of the undirected graph  $G$  defined in section II with positive line weights  $B_{ij} \cos(\theta_i - \theta_j)$ . Hence  $\bar{L}$  is semi-positive definite and all its principle minors are nonsingular [5]. In the coordination of  $\varphi$ , we define function

$$U(\varphi) = \sum_{(i,j) \in \mathcal{E}} B_{ij} (1 - \cos(\varphi_i - \varphi_j)), \quad (23)$$

with Hessian matrix

$$L = \begin{pmatrix} B_{22} & -B_{23} \cos(\varphi_{23}) & \dots & -B_{2n} \cos(\varphi_{2n}) \\ -B_{32} \cos(\varphi_{32}) & B_{33} & \dots & -B_{3n} \cos(\varphi_{3n}) \\ \vdots & \vdots & \ddots & \vdots \\ -B_{n2} \cos(\varphi_{n2}) & -B_{n3} \cos(\varphi_{n3}) & \dots & B_{nn} \end{pmatrix}, \quad (24)$$

where  $B_{ii} = \sum_{j \in \mathcal{V}} B_{ij} \cos(\varphi_{ij})$ ,  $\varphi_{ij} = \varphi_i - \varphi_j$ , and  $\varphi_1 = 0$ . Note that  $B_{ij} \cos(\varphi_{ij}) = B_{ij} \cos(\theta_{ij})$ , thus  $L$  is a principle minor of  $\bar{L}$  and is nonsingular. Hence the Jacobian of (21d) with respect to  $\varphi_P$ , which is a principle minor of  $L$ , is nonsingular.

Second, because  $J_i$  is strictly convex as in Assumption 3 such that  $J_i'' > 0$ , we obtain  $(J_i^{-1})' = \frac{1}{J_i''} > 0$  which yields  $(\sum_{i \in \mathcal{V}_K} J_i^{-1}(\lambda))' > 0$ . Hence (21f) is nonsingular.  $\square$

What follows is the proof of Theorem 5.1 with the Lyapunov/LaSalle stability criterion.

*Proof of Theorem 5.1:* Lemma 5.2 and Assumption 5 states that the equilibrium state  $z^* = (\varphi^*, \omega_M^*, \eta^*, \lambda^*) \in \Psi$  is unique. The proof of the statement (b) in Theorem 5.1 is based on Theorem A.1. Consider an incremental Lyapunov function candidate

$$V(\varphi, \omega_M, \eta, \lambda) = V_1 + \alpha V_2 + V_3. \quad (25)$$

where  $V_1$  is the classical energy-based function [6]

$$V_1(\varphi, \omega_M) = U(\varphi) - U(\varphi^*) - \nabla_\varphi U(\varphi^*)(\varphi - \varphi^*) + \frac{1}{2} \omega_M^T M_M \omega_M,$$

and  $V_2, V_3$  are positive definite functions

$$V_2(\lambda) = \frac{1}{2} \left( \sum_{i \in \mathcal{V}_K} J_i^{-1}(\lambda) - \sum_{i \in \mathcal{V}_K} J_i^{-1}(\lambda^*) \right)^2,$$

$$V_3(\omega_M, \eta) = \frac{k^2}{2} \left( \sum_{i \in \mathcal{V}_M} M_i \omega_i + \eta - \eta^* \right)^2.$$

Note that the definition of  $U(\varphi)$  is in (23) and  $V_2 = V_3$  by (21f).  $V_3$  is introduced to involve in the state variable  $\eta$  to the Lyapunov function.

First, we prove that  $\dot{V} \leq 0$ . From the dynamic system (21) and the definition of  $V_1$ , it yields that

$$\dot{V}_1 = - \sum_{i \in \mathcal{V}_M \cup \mathcal{V}_F} D_i \omega_i^2 + \sum_{i \in \mathcal{V}_K} \omega^T (J_i^{-1}(\lambda) - J_i^{-1}(\lambda^*)), \quad (27)$$

by (21f), we derive

$$\begin{aligned} \dot{V}_2 &= -k \left[ \sum_{i \in \mathcal{V}_K} J_i^{-1}(\lambda) - \sum_{i \in \mathcal{V}_K} J_i^{-1}(\lambda^*) \right] \left[ \sum_{i \in \mathcal{V}_M} M_i \dot{\omega}_i + \dot{\eta} \right] \\ &\quad \text{by summing (21b-21e)} \\ &= -k \left[ \sum_{i \in \mathcal{V}_K} J_i^{-1}(\lambda) - \sum_{i \in \mathcal{V}_K} J_i^{-1}(\lambda^*) \right] \left[ \sum_{i \in \mathcal{V}} P_i + \sum_{i \in \mathcal{V}_K} J_i^{-1}(\lambda) \right] \\ &\quad \text{by (22b)} \\ &= -k \left[ \sum_{i \in \mathcal{V}_K} J_i^{-1}(\lambda) - \sum_{i \in \mathcal{V}_K} J_i^{-1}(\lambda^*) \right]^2, \end{aligned} \quad (28a)$$

by expanding the quadratic

$$\begin{aligned} &= -k \sum_{i \in \mathcal{V}_K} [J_i^{-1}(\lambda) - J_i^{-1}(\lambda^*)]^2 \\ &\quad - 2k \sum_{i \neq j, i, j \in \mathcal{V}_K} [J_i^{-1}(\lambda) - J_i^{-1}(\lambda^*)] [J_j^{-1}(\lambda) - J_j^{-1}(\lambda^*)] \\ &\quad \text{by Newton-Leibniz formula} \\ &= -k \sum_{i \in \mathcal{V}_K} [J_i^{-1}(\lambda) - J_i^{-1}(\lambda^*)]^2 \\ &\quad - 2k \sum_{i \neq j, i, j \in \mathcal{V}_K} \left[ \int_{\lambda^*}^{\lambda} (J_i^{-1})' ds \right] \left[ \int_{\lambda^*}^{\lambda} (J_j^{-1})' ds \right]. \end{aligned} \quad (28b)$$

and by  $V_3 = V_2$  and (28a), we obtain

$$\dot{V}_3 = -k \left[ \sum_{i \in \mathcal{V}_K} (J_i^{-1}(\lambda) - J_i^{-1}(\lambda^*)) \right]^2. \quad (29)$$

Hence, with (27, 28b, 29), we derive

$$\begin{aligned} \dot{V} &= - \sum_{i \in \mathcal{V}_M \cup \mathcal{V}_F} D_i \omega_i^2 + \sum_{i \in \mathcal{V}_K} \omega^T [J_i^{-1}(\lambda) - J_i^{-1}(\lambda^*)] \\ &\quad - k \alpha \sum_{i \in \mathcal{V}_K} [J_i^{-1}(\lambda) - J_i^{-1}(\lambda^*)]^2 \\ &\quad - k \alpha \sum_{i \neq j, i, j \in \mathcal{V}_K} \left[ \int_{\lambda^*}^{\lambda} (J_i^{-1})' ds \right] \left[ \int_{\lambda^*}^{\lambda} (J_j^{-1})' ds \right] \\ &\quad - k \left[ \sum_{i \in \mathcal{V}_K} J_i^{-1}(\lambda) - \sum_{i \in \mathcal{V}_K} J_i^{-1}(\lambda^*) \right]^2 \\ &= - \sum_{i \in \mathcal{V}_K} \frac{D_i}{2} \omega_i^2 - \sum_{i \in \mathcal{V}_K} \frac{D_i}{2} \left[ \omega_i - \frac{J_i^{-1}(\lambda) - J_i^{-1}(\lambda^*)}{D_i} \right]^2 \\ &\quad - \sum_{i \in \mathcal{V}_K} \left[ k \alpha - \frac{1}{2D_i} \right] [J_i^{-1}(\lambda) - J_i^{-1}(\lambda^*)]^2 - \\ &\quad - 2k \alpha \sum_{i \neq j, i, j \in \mathcal{V}_K} \left[ \int_{\lambda^*}^{\lambda} (J_i^{-1})' ds \right] \left[ \int_{\lambda^*}^{\lambda} (J_j^{-1})' ds \right] \\ &\quad - k \left[ \sum_{i \in \mathcal{V}_K} J_i^{-1}(\lambda) - \sum_{i \in \mathcal{V}_K} J_i^{-1}(\lambda^*) \right]^2 - \sum_{i \in \mathcal{V}_M \cup \mathcal{V}_F / \mathcal{V}_K} D_i \omega_i^2 \end{aligned}$$

where the equation

$$\sum_{i \in \mathcal{V}_M \cup \mathcal{V}_F} D_i \omega_i^2 = \sum_{i \in \mathcal{V}_K} D_i \omega_i^2 + \sum_{i \in \mathcal{V}_M \cup \mathcal{V}_F / \mathcal{V}_K} D_i \omega_i^2$$

is used due to the fact that  $\mathcal{V}_K \subset \mathcal{V}_M \cup \mathcal{V}_F$ .

Since  $J_i(u_i)$  is strictly convex and  $(J_i^{-1})' = \frac{1}{J_i''} > 0$ , we derive

$$k \alpha \sum_{i \neq j, i, j \in \mathcal{V}_K} \left[ \int_{\lambda^*}^{\lambda} (J_i^{-1})' ds \right] \left[ \int_{\lambda^*}^{\lambda} (J_j^{-1})' ds \right] > 0,$$



Thus by setting  $\alpha > \frac{1}{kD_i}$ , we obtain  $\dot{V} \leq 0$ .

Second, we prove that  $z^* = (\varphi^*, \omega_M^*, \eta^*, \lambda^*)$  is a strict minimum of  $V(\varphi, \omega_M, \eta, \lambda)$  such that  $\nabla V|_{z^*} = 0$  and  $\nabla^2 V|_{z^*} > 0$ . It can be easily verified that  $V|_{z^*} = 0$  and

$$\nabla V|_{z^*} = \text{col}(\nabla_\varphi V, \nabla_{\omega_M} V, \nabla_\eta V, \nabla_\lambda V)|_{z^*} = 0 \in \mathbb{R}^{n+n_M+1}$$

where

$$\begin{aligned} \nabla_\varphi V &= \nabla_\varphi U - \nabla_\varphi U^*, \\ \nabla_{\omega_M} V &= M\omega_M + M(k^2(\sum_{i \in \mathcal{V}_M} M_i \omega_i + \eta - \eta^*))1_{n_M}), \\ \nabla_\eta V &= k^2(\sum_{i \in \mathcal{V}_M} M_i \omega_i + \eta - \eta^*), \\ \nabla_\lambda V &= \alpha \left( \sum_{i \in \mathcal{V}_K} J_i'^{-1}(\lambda) - \sum_{i \in \mathcal{V}_K} J_i'^{-1}(\lambda^*) \right) \left( \sum_{i \in \mathcal{V}_K} J_i'^{-1}(\lambda) \right)'. \end{aligned}$$

Here  $k^2(\sum_{i \in \mathcal{V}_M} M_i \omega_i + \eta - \eta^*)1_{n_M}$  is a vector with all components equal to  $k^2(\sum_{i \in \mathcal{V}_M} M_i \omega_i + \eta - \eta^*)$ . The Hessian matrix of  $V$  is

$$\nabla^2 V|_{z^*} = \text{blkdiag}(L, H, \Lambda),$$

which is a block diagonal matrix with block matrices  $L, H$ , and  $\Lambda$ .  $L$  is positive definite by (24),

$$\Lambda = \alpha \left( \left( \sum_{i \in \mathcal{V}_K} J_i'^{-1}(\lambda^*) \right)' \right)^2 > 0$$

which is a scalar value, and  $H$  is the Hessian matrix of the function

$$\bar{V} = \frac{1}{2} \omega_M^T M_M \omega_M + \frac{k^2}{2} \left( \sum_{i \in \mathcal{V}_M} M_i \omega_i + \eta - \eta^* \right)^2$$

which is positive definite for any  $(\omega_M, \eta)$ , thus  $H$  is positive definite. Hence, we have proven that  $z^*$  is a strict minimum of  $V$ .

Finally, we prove that the invariant set

$$\{(\varphi, \omega_M, \eta, \lambda) | \dot{V}((\varphi, \omega_M, \eta, \lambda)) = 0\}$$

contains only the equilibrium point.  $\dot{V} = 0$  implies that  $\{\omega_i = 0, i \in \mathcal{V}_M \cup \mathcal{V}_F\}$ . Hence  $\{\varphi_i, i \in \mathcal{V}\}$  are constants. By lemma 5.2, there is at most one equilibrium with  $\varphi \in \Phi$ . In this case,  $z^*$  is the only one equilibrium in the neighborhood of  $z^*$ , i.e.,  $\Psi^d = \{(\varphi, \omega_M, \eta, \lambda) | V(\varphi, \omega_M, \eta, \lambda) \leq c, \varphi \in \Phi\}$  for some  $c > 0$ . Hence with any initial state  $z^0$  that satisfies the algebraic equations (21d) and (21f), the trajectory converges to the equilibrium state  $z^*$ .  $\square$

## VI. SIMULATIONS OF THE CLOSED-LOOP SYSTEM

In this section, we evaluate the performance of the PIAC method on the IEEE New England power grid shown in Fig. 1. The data are obtained from [3]. In the test system, there are 10 generators, and 39 buses and it serves a total load of about 6 GW. The voltage at each bus is a constant which is obtained by power flow calculation with PSAT [18]. In the network, there actually are 49 nodes, i.e., 10 nodes for the generators, 39 nodes for the buses. Each synchronous machine is connected to a bus and its phase angle is rigidly tied to the rotor

angle of the bus if the voltages of the system are constants, e.g., the classical model of synchronous machines [13]. We simplify the test system to a system of 39 nodes by considering the generator and the bus as one node. This is reasonable because the angles of the synchronous machine and the bus have the same dynamics. The 10 generators are in the set  $\mathcal{V}_M = \{30, 31, 32, 33, 34, 35, 36, 37, 38, 39\}$  and the other buses are in the set  $\mathcal{V}_F$  which are assumed to be frequency dependent loads. The controllers are installed at the 10 generator nodes, i.e.,  $\mathcal{V}_K = \mathcal{V}_M$ . The buses in  $\mathcal{V}_M \cup \mathcal{V}_F$  and controllers in  $\mathcal{V}_K$  are connected by a communication network. The droop control coefficient  $D_i = 1$  pu,  $i \in \mathcal{V}_F \cup \mathcal{V}_M$ . As in [9], without loss of generality, we consider the quadratic cost functions  $J_i(u_i) = u_i^2/\alpha_i$ ,  $i \in \mathcal{V}_K$  which measures the cost money of the controller at node  $i$ . The economic dispatch coefficients  $\alpha_i$  are generated randomly with a uniform distribution on  $(0, 1)$ .

In the simulations, the system is initially at a supply-demand balanced state with 60 Hz frequency. At time  $t = 0.5$  second, a step-wise increase of 33 MW of the loads at each of the buses 4, 12, and 20, amounting to a total power imbalance of 99 Mw, causes the frequency to drop below the nominal frequency.

We first evaluate the performance of PIAC on the network which is assumed as a single area and compare it with the Gather-Broadcast control method. Then we implement the PIAC method in the network separated into two areas and show that the control actions of the areas are totally decoupled by PIAC as described in the subsection IV-B.

### A. Numerical results of the Single-area implementation

In this subsection, the network is seen as a single area. We evaluate the performance of PIAC by comparing with the Gather-Broadcast control method.

The control gain  $k = 10$  for PIAC method and  $k_{GB} = 60$  for the Gather-Broadcast control method respectively. Note that a smaller  $k_{GB}$  leads to larger frequency deviations and a larger one leads to a more serious overshoot of control inputs. The coefficient in (11)  $C_i = 1/N$  for all controllers for Gather-Broadcast control. We use the Euler-Forward method to discretize the ordinary differential equations and use the Newton-Raphson method to solve the nonlinear system.

Fig. 2a and Fig. 2b show the frequency response of the two control method at buses 30, 31, 32, 33, and 34,

which indicate that both the PIAC method and Gather-Broadcast method can restore the nominal frequency. However, the frequency deviation under the PIAC method is much smaller than under the Gather-Broadcast method which introduces extra oscillations to the frequency. This is because the control inputs of the Gather-Broadcast method overshoot the desired value as Fig. 2d shows, while the ones of the PIAC method converges exponentially as Fig. 2c shows. Since the economic power dispatch is solved on line, it can be observed in Fig. 2e that the marginal cost of all the controllers is the same during the transient phase under the control of PIAC. This is the same as for the control of Gather-Broadcast method.

We remark that the larger the gain of the Gather-Broadcast control method the larger are the oscillations of frequency

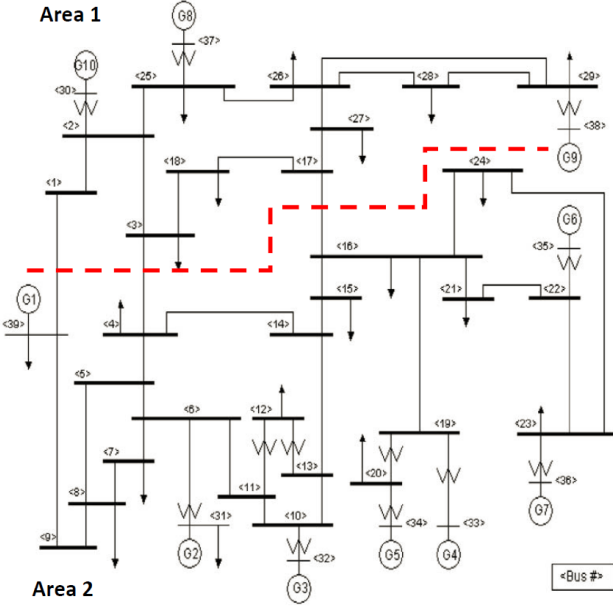


Fig. 1. IEEE New England test power system.

deviations even though the frequencies converge to the nominal frequency faster. However, the control inputs of the PIAC method converge to the power imbalance faster under larger control gain  $k$ , which leads to smaller frequency deviations.

### B. Numerical results of the Multi-area implementation

In this subsection, the network is separated into two areas by the red dashed line. All the parameters of the controllers are the same to the ones in the single-area implementation. There are 3 generators in area  $A_1$  and 7 generators in the area  $A_2$  i.e.,  $\mathcal{V}_{M_1} = \{30, 37, 38\}$ ,  $\mathcal{V}_{M_2} = \{31, 32, 33, 34, 35, 36, 39\}$ . The boundary lines of the area  $A_1$  are in  $\mathcal{E}_{A_1} = \{(1, 39), (3, 4), (17, 16)\}$ . As in the previous subsection VI-A, the secondary frequency controllers are installed at the nodes of the generators. After the step-wise increase of the loads in the area  $A_2$ , the multi-area implementation of PIAC recovers the nominal frequency as Fig. 3a shows and the power export deviation of the area  $A_1$  converges to zero as the black dashed lines shows in Fig. 3b. Fig. 3b also shows that as the system converges to a new state, the power flows in the three line in  $\mathcal{E}_{A_1}$  are different from the ones before the step-wise increase of the loads in area  $A_2$ .

A characteristic of PIAC is that it decouples the control actions of the areas, which can be observed in Fig. 3c. Since the step-wise increase of the power loads at the buses 4, 12 and 30 happen in the area  $A_2$ , the control inputs of the area  $A_1$  are zero and the power is balanced by the controllers in the area  $A_2$ . This shows that with the PIAC method, the power can be balanced locally in an area without influencing to its neighbors. Furthermore, Fig. 3d shows that the marginal costs of the controllers in one area are the same during the transient phase which is the same as in the single-area implementation of PIAC.

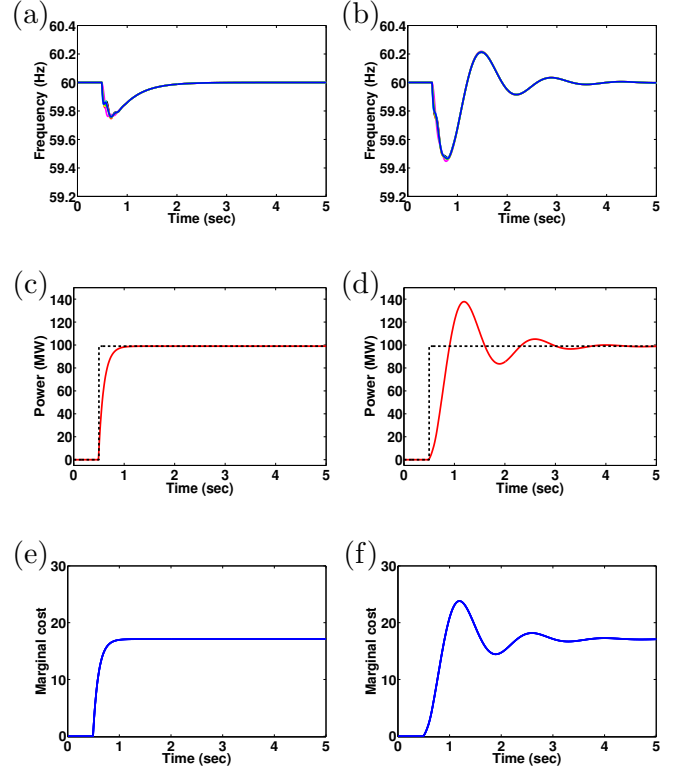


Fig. 2. The single area implementation of PIAC compared with Gather-broadcast method. The figures in the left column are the result of PIAC and the ones in the right column are the result of Gather-broadcast method. (a-b) Frequency response of the generators  $\{30, 31, 32, 33\}$ . (c-d) The total control inputs of the controllers. The black dashed lines denote the power imbalance of the network. (e-f) The marginal cost of all the controllers.

## VII. CONCLUSION

In this paper, we proposed a secondary frequency control approach, named PIAC, to restore the nominal frequency of power systems with a minimized control cost. A main feature of PIAC is that the estimated power imbalance converges exponentially in a speed that only depends on a gain coefficient and the gain coefficient can be tuned according to the sensitivity of the control devices. Hence PIAC eliminates the drawback of the traditional integral control based secondary frequency control approach, in which large control gain coefficients lead to an overshoot problem of the control inputs and small ones result in a large frequency deviation of the power systems. When implemented in a network with multiple areas, PIAC decouples the control actions of the areas such that the power supply and demand of an area can be balanced locally in the area without any influences to the neighbors. For the power systems with a large amount of integrated renewable energy, the large transient frequency deviation can be reduced by PIAC with advanced control devices and communication networks.

However, in practice, there is usually some noise from the measurement of frequency and time delays and even information losses in the communication. In addition, the resistance of the transmission lines can not be neglected in some power networks. Hence, further investigation on the performance of PIAC on such a lossy power network with

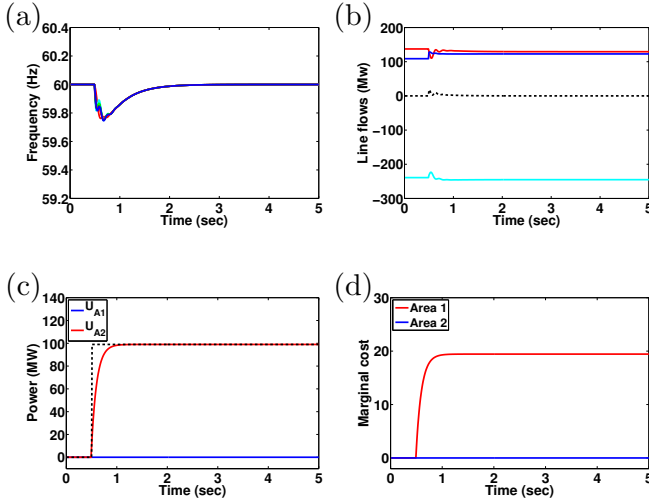


Fig. 3. Multi-area control of PIAC. (a) The frequency response of all the generators. (b) The line flows in the boundary lines, i.e., (1,39), (3,4), and (17,16). (c) The control inputs of the generators in area 1 and area 2. The black dashed line is the power imbalance of the network. (d) The marginal cost of the controllers in area 1 and area 2.

noisy measurements and time delays is needed.

#### APPENDIX PRELIMINARIES ON DAE SYSTEMS

Consider the following DAE systems

$$\dot{x} = f(x, y), \quad (31a)$$

$$0 = g(x, y). \quad (31b)$$

where  $x \in \mathbb{R}^n, y \in \mathbb{R}^m$  and  $f : \mathbb{R}^n \times \mathbb{R}^m \rightarrow \mathbb{R}^n$  and  $g : \mathbb{R}^n \times \mathbb{R}^m \rightarrow \mathbb{R}^m$  are twice continuously differentiable functions.  $(x(x_0, y_0, t), y(x_0, y_0, t))$  is the solution with the admissible initial conditions  $(x_0, y_0)$  satisfying the algebraic constraints

$$0 = g(x_0, y_0). \quad (32)$$

and the maximal domain of a solution of (31) is denoted by  $I \subset \mathbb{R}_{\geq 0}$  where  $\mathbb{R}_{\geq 0} = \{x \in \mathbb{R} | x \geq 0\}$ .

Before presenting the Lyapunov/LaSalle stability criterion of the DAE system, we make the following two assumptions.

**Assumption A.2:** The DAE system possesses an equilibrium state  $(x^*, y^*)$  such that  $f(x^*, y^*) = 0, g(x^*, y^*) = 0$ .

**Assumption A.3:** Let  $\Omega \subseteq \mathbb{R}^n \times \mathbb{R}^m$  be an open connected set containing  $(x^*, y^*)$ , assume (31b) is *regular* such that the Jacobian of  $g$  with respect to  $y$  is a full rank matrix for any  $(x, y) \in \Omega$ , i.e.,

$$\text{rank}(\nabla_y g(x, y)) = m, \quad \forall (x, y) \in \Omega.$$

Assumption A.3 ensures the existence and uniqueness of the solutions of (31) in  $\Omega$  over the interval  $I$  with the initial condition  $(x_0, y_0)$  satisfying (32).

The following theorem provides a sufficient stability criterion of the equilibrium of DAE in (31).

**Theorem A.1:** (Lyapunov/LaSalle stability criterion [20], [12]): Consider the DAE system in (31) with assumptions A.2

and A.3, and an equilibrium  $(x^*, y^*) \in \Omega_H \subset \Omega$ . If there exists a continuously differentiable function  $H : \Omega_H \rightarrow \mathbb{R}$ , such that  $(x^*, y^*)$  is a strict minimum of  $H$  i.e.,  $\nabla H|_{(x^*, y^*)} = 0$  and  $\nabla^2 H|_{(x^*, y^*)} > 0$ , and  $\dot{H}(x, y) \leq 0, \forall (x, y) \in \Omega_H$ , then the following statements hold:

(1).  $(x^*, y^*)$  is a stable equilibrium with a local Lyapunov function  $V(x, y) = H(x, y) - H(x^*, y^*) \geq 0$  for  $(x, y)$  near  $(x^*, y^*)$ ,

(2). Let  $\Omega_c = \{(x, y) \in \Omega_H | H(x, y) \leq c\}$  be a compact sub-level set for some  $c > H(x^*, y^*)$ . If no solution can stay in  $\{(x, y) \in \Omega_c | \dot{H}(x, y) = 0\}$  other than  $(x^*, y^*)$ , then  $(x^*, y^*)$  is asymptotically stable.

We refer to [20] and [12] for the proof of Theorem A.1.

#### ACKNOWLEDGMENT

The authors thank Prof. Chen Shen from Tsinghua University for his valuable discussions on the background of the frequency control of power systems and useful advices on the simulations. Kaihua Xi thanks the China Scholarship Council for the financial support.

#### REFERENCES

- [1] M. Andreasson, D. V. Dimarogonas, H. Sandberg, and K. H. Johansson. Distributed control of networked dynamical systems: Static feedback, integral action and consensus. *IEEE Transactions on Automatic Control*, 59(7):1750–1764, Jul. 2014.
- [2] A. Arapostathis, S. Sastry, and P. Varaiya. Analysis of power-flow equation. *International Journal of Electrical Power & Energy Systems*, 3(3):115–126, Jul. 1981.
- [3] T. Athay, R. Podmore, and S. Virmani. A practical method for the direct analysis of transient stability. *IEEE Transactions on Power Apparatus and Systems*, PAS-98(2):573–584, 1979.
- [4] S. Boyd, N. Parikh, E. Chu, B. Peleato, and J. Eckstein. Distributed optimization and statistical learning via the alternating direction method of multipliers. *Foundations and Trends in Machine Learning*, 3(1):1–122, 2010.
- [5] R. A. Brualdi and H. J. Ryser. *Combinatorial matrix theory*, volume 39. Cambridge University Press, 1991.
- [6] C. De Persis and N. Monshizadeh. Bregman storage functions for microgrid control. *arXiv preprint, arXiv: 1510.05811*, 2016.
- [7] L. Dong, Y. Zhang, and Z. Gao. A robust decentralized load frequency controller for interconnected power systems. *ISA Transactions*, 51(3):410–419, 2012.
- [8] F. Dörfler and F. Bullo. Synchronization and transient stability in power networks and nonuniform Kuramoto oscillators. *SIAM Journal on Control and Optimization*, 50(3):1616–1642, Jan. 2012.
- [9] F. Dörfler and S. Grammatico. Gather-and-broadcast frequency control in power systems. *submitted*, 2016.
- [10] F. Dörfler, J. W. Simpson-Porco, and F. Bullo. Breaking the hierarchy: distributed control and economic optimality in microgrids. *IEEE Transactions on Control of Network Systems*, 3(3):241–253, Sep. 2016.
- [11] J. Han. From PID to active disturbance rejection control. *IEEE Transactions on Industrial Electronics*, 56(3):900–906, 2009.
- [12] D. J. Hill and I. M. Y. Mareels. Stability theory for differential algebraic systems with applications to power systems. *IEEE Trans. Circuits and Systems*, 37(11):1416–1423, 1990.
- [13] M.D. Ilić and J. Zaborsky. *Dynamics and control of large electric power systems*. John Wiley & Sons, 2000.
- [14] P. Kundur. *Power system stability and control*. McGraw-Hill, 1994.
- [15] N. Li, C. Zhao, and L. Chen. Connecting automatic generation control and economic dispatch from an optimization view. *IEEE Transactions on Control of Networked Systems*, 3(3):254–263, 2016.
- [16] F. Liu, Y. H. Song, J. Ma, S. Mei, and Q. Lu. Optimal load-frequency control in restructured power systems. *IEE Proceedings - Generation, Transmission and Distribution*, 150(1):87–95, 2003.
- [17] Y. Liu, Z. Qu, H. Xin, and D. Gan. Distributed real-time optimal power flow control in smart grid. *IEEE Transactions on Power Systems*, 8950(c):1–1, 2016.

- [18] F. Milano. *Power systems analysis toolbox*. University of Castilla, Castilla-La Mancha, Spain, 2008.
- [19] P. Schavemaker and L. van der Sluis. *Electrical power system essentials*. John Wiley & Sons, 2008.
- [20] J. Schiffer and F. Dörfler. On stability of a distributed averaging PI frequency and active power controlled differential-algebraic power system model. In *European Control Conference*, 2016.
- [21] J. Schiffer, T. Seel, J. Raisch, and T. Sezi. Voltage stability and reactive power sharing in inverter-based microgrids with consensus-based distributed voltage control. *IEEE Transactions on Control Systems Technology*, 24(1):96–109, 2016.
- [22] J. W. Simpson-Porco, F. Dörfler, and F. Bullo. Voltage collapse in complex power grids. *Nature Communications*, 7:10790, 2016.
- [23] A. J. Wood and B. F. Wollenberg. *Power generation, operation, and control*. John Wiley & Sons, 2nd edition, 1996.
- [24] X. Wu, F. Dorfler, and M. R. Jovanovic. Input-Output analysis and decentralized optimal control of inter-area oscillations in power systems. *IEEE Transactions on Power Systems*, 31(3):2434–2444, May 2016.
- [25] X. Wu and C. Shen. Distributed optimal control for stability enhancement of microgrids with multiple distributed generators. *IEEE Transactions on Power Systems*, 8950(c):1–1, 2017.
- [26] X. Wu, C. Shen, and R. Iravani. A distributed, cooperative frequency and voltage control for microgrids. *IEEE Transactions on Smart Grid*, 3053(c):1–1, 2016.
- [27] K. Xi, J. L. A. Dubbeldam, and H. X. Lin. Synchronization of cyclic power grids: equilibria and stability of the synchronous state. *Chaos: An Interdisciplinary Journal of Nonlinear Science*, 27(1):013109, Jan. 2017.
- [28] K. Xi, J. L. A. Dubbeldam, H. X. Lin, and J. H. van Schuppen. Power imbalance allocation control for secondary frequency control of power systems. *To appear in Proc. of IFAC 2017 World Congress, Toulouse, France*, 2017.
- [29] K. Xi, H. X. Lin, and J. H. van Schuppen. Power imbalance allocation control of frequency control of power systems with time-varying power imbalance. *Submitted to China Control Conference 2017*, 2016.
- [30] C. Zhao, M. Enrique, S. H. Low, and J. Bialek. A unified framework for frequency control and congestion management. *submitted*, 2016.
- [31] C. Zhao, E. Mallada, and F. Dörfler. Distributed frequency control for stability and economic dispatch in power networks. Chicago, 2015. In *American Control Conference*.
- [32] C. Zhao, U. Topcu, N. Li, and S. Low. Design and stability of load-side primary frequency control in power systems. *IEEE Transactions on Automatic Control*, 59(5):1177–1189, May 2014.